Supplemental Material:

Similar Endothelial Glycocalyx Structures in Microvessels from a Range of Mammalian Tissues: Evidence for a Common Filtering Mechanism?

K. P. Arkill, C. Knupp, C. C. Michel, C. R. Neal, K. Qvortrup, J Rostgaard, and J. M. Squire

Staining of the Glycocalyx by the Rostgaard Method(1-3)

Following induction of surgical anaesthesia, the animal's trachea was cannulated to facilitate adequate artificial ventilation. A self-retaining cannula was inserted into the left ventricle of the heart and clamped tightly. The cannula consisted of two barrels. The outer barrel was connected to a peristaltic pump which delivered the fixative (2% glutaraldehyde and 13.3% oxygenated fluorocarbon in 0.05M sodium phosphate buffer at pH 7.4). The inner barrel was connected to a pressure transducer that monitored the perfusion pressure, directing the pump to deliver the perfusate at a steady pressure of 100 mm Hg. The caudal caval vein was severed immediately before the perfusion was initiated.. After fixation, small specimen blocks (1 mm^3) were trimmed, rinsed in 0.12 M sodium cacodylate buffer (pH 7.4) for 1 h, postfixed in 1% OsO_4 in 0.1 M cacodylate buffer (pH 7.4) for 2 h, very briefly rinsed (10-20 sec) in 0.15 M sodium cacodylate buffer (pH 7.4), rinsed in distilled water and treated with 1% tannic acid in distilled water for 3 h. They were then stained *en bloc* in 1% uranyl acetate in distilled water overnight, rinsed in distilled water and dehydrated in 70%, 96% and 100% ethanol. The specimens were transferred to propylene oxide and embedded in Epon according to standard procedures. Ultrathin sections of approximately 80nm were cut with a Reichert-Jung Ultracut E microtome and collected with Formvar support films on copper slot grids, stained with uranyl acetate and lead citrate, and examined and imaged with a Philips EM-400 electron microscope operated at 60 kV accelerating voltage or a Philips EM-208 electron microscope operated at an accelerating voltage of 70 kV.

Demonstration of the Autocorrelation Technique Used

The underlying lattices are not very clear in supplemental figure 1 (noise added column), but a clear lateral spacing is evident in the autocorrelation (AC). Each image segment had a border added (1/35 of the original dimensions), in which the border intensity tapered to the mean density of the image segment to avoid inducing edge effects. An AC was then performed on the Fast Fourier Transform of the image segment using ImageJ. Due to the finite size of a computational AC, the correlation of a large object can go off one side of the image and reappear on the other. To avoid this aliasing issue, an intensity profile only 0.75 of the AC image diameter was taken horizontally through the center line of the AC. The profiles from micrographs of many different magnifications were mapped using linear interpolation to an array representing 1nm per unit and scaled so that the maximum relative intensity was 10,000. Finally a constant linear background was subtracted to zero the observed minimum. This typically gave a range of intensities of the order of 100s.

Expressions for partition coefficient of a spherical molecule in a square matrix when ($r + a) > b/2$.

Supplemental Figure 2A represents an idealised square unit of the glycocalyx of side length b as seen from above. The unit has been divided into four quadrants of side length $b/2 = l$. Let the radius of each cylindrical fiber at the corners of the matrix be r and the radius of a spherical molecule be a.

In the lower left-hand quadrant, the circle centered over the corner of the unit square represents the cross-section of one of the cylindrical fibers that define the unit. The shorter arc within represents the edge of the fiber (radius=*r*) and the larger arc has a radius *(r+a)* and defines the path of the center of a spherical molecule of radius *a,* when it is in contact with the fiber. The area AS is the available space for the solute molecule (radius a) within the quadrant.

Fraction of the total area from which the center of the molecule is excluded is $V_{x:}$

$$V_X = \frac{l.x + 0.5.(\pi/2 - 2\theta).(r+a)^2}{l^2},$$

where $x = \sqrt{(r+a)^2 - l^2}$

and $\theta = \sin^{-1}\left(x/(r+a)\right)$.

Fractional area available to solute: $F_S = 1 - V_x$

Fraction of the total area available for water molecules, F_W:

$$F_W = 1 - \frac{\pi.r^2}{4.l^2},$$

Partition coefficient, λ, of solute between open solution and solution within the matrix:

$$\lambda = \frac{F_S}{F_W}.$$

Expressions for partition coefficient of a spherical molecule in a square matrix when (*r* + *a)* ≤ *b*/2:

$$\lambda = \frac{F_S}{F_W}.$$

as before, but:

$$F_S = 1 - \frac{\pi.(r+a)^2}{4.l^2},$$

Expressions for partition coefficient of a spherical molecule in a hexagonal matrix when (*r* + *a)* > *b/2*.

The expression can be derived in a similar way to the square lattice but using a triangle as in supplemental figure 2B.

$$F_W = 1 - \frac{\pi.r^2}{6.l^2 Tan(\pi/6)}$$

$$V_X = \frac{l.x + 0.5.(\pi/3 - 2\theta).(r+a)^2}{l^2 Tan(\pi/6)}$$

Expressions for partition coefficient of a spherical molecule in a hexagonal matrix when ($r + a$) ≤ $b/2$

$$F_S = 1 - \frac{\pi.(r+a)^2}{6.l^2 Tan(\pi/6)}$$

This expression is the equivalent of that derived by Zhang et al (4).

Figure Captions:

Supplemental Figure 1: Using Autocorrelation (AC) to find fiber spacings in an example model. An obscured area of fiber matrix was developed using dots to represent fiber centers, these were generated with stochastic error on a repeating lattice (102 horizontal pixel spacing) three times (rows A,B and C, left images) and then overlaid with random dots (middle images). The AC of each noisy image was performed to find any predominant underlying spacings (right images). To find the horizontal spacings the AC intensity profiles through a line P was plotted for the three examples. The center point has maximum correlation due to all the dots being correlated but spacings can be measured directly from the center to peaks in the profile. Using Peakfit (Jandel) to find the peaks in the AC, a frequency distribution (D) normalised to the number of fits and smoothed with a triangular smoothing function can be generated (see methods for protocol) . The arrows point to the expected frequency distribution maxima from a pure lattice. The frequency distribution from just these three profiles (dotted line) makes the correct maxima apparent, but with a further seven profiles (solid line) the correct lattice spacing is shown with the maxima from the noise greatly suppressed.

Supplemental Figure 2: Diagrams to aid in the derivation of the Partition coefficient of a solute between open solution and solution. (A) The proportion of available space (AS) in a proportion bound by '*l*' for a square lattice for a molecule radius a. ***b*** is the center to center fiber spacing. (B) The equivalent diagram for a Hexagonally packed system.

Supplementary References

1. Rostgaard, J., and K. Qvortrup. 1997. Electron microscopic demonstrations of filamentous molecular sieve plugs in capillary fenestrae. Microvascular Research 53:1-13.
2. Rostgaard, J., and K. Qvortrup. 2002. Sieve plugs in fenestrae of glomerular capillaries - site of the filtration barrier? Cells Tissues Organs 170:132-138.
3. Rostgaard, J., K. Qvortrup, and S. S. Poulsen. 1993. Improvements in the technique of vascular perfusion-fixation employing a fluorocarbon-containing perfusate and a peristaltic pump controlled by pressure feedback. Journal of Microscopy-Oxford 172:137-151.
4. Zhang, X. B., F. R. Curry, and S. Weinbaum. 2006. Mechanism of osmotic flow in a periodic fiber array. American Journal of Physiology-Heart and Circulatory Physiology 290:H844-H852.

Supplementary Figure 1

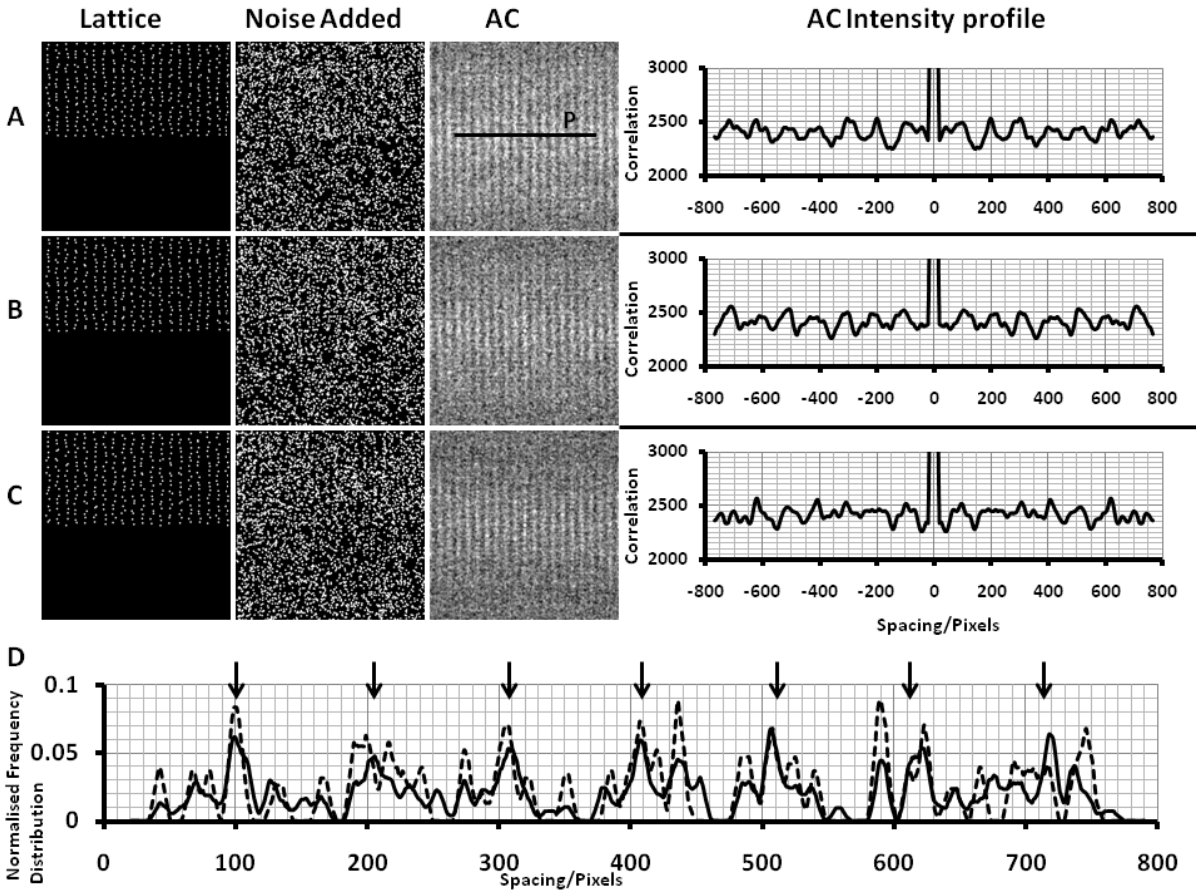

Supplementary Figure 2